



Published in final edited form as:

Nat Astron. 2018 ; 2: 260–213. doi:10.1038/s41550-017-0377-9.

Surface clay formation during short-term warmer and wetter conditions on a largely cold ancient Mars

Janice L. Bishop^{1,2,*}, Alberto G. Fairén^{3,4}, Joseph R. Michalski⁵, Luis Gago-Duport⁶, Leslie L. Baker⁷, Michael A. Velbel^{8,9}, Christoph Gross¹⁰, Elizabeth B. Rampe¹¹

¹SETI Institute, Mountain View, CA, USA.

²National Aeronautics and Space Administration's Ames Research Center, Moffett Field, CA, USA.

³Centro de Astrobiología (Consejo Superior de Investigaciones Científicas-Instituto Nacional de Técnica Aeroespacial), Madrid, Spain.

⁴Cornell University, Ithaca, NY, USA.

⁵Department of Earth Sciences & Laboratory for Space Research, University of Hong Kong, Hong Kong, China.

⁶University of Vigo, Vigo, Spain.

⁷University of Idaho, Moscow, ID, USA.

⁸Michigan State University, East Lansing, MI, USA.

⁹Smithsonian Institution, Washington, DC, USA.

¹⁰Freie Universität Berlin, Berlin, Germany.

¹¹National Aeronautics and Space Administration-Johnson Space Center, Houston, TX, USA.

Abstract

The ancient rock record for Mars has long been at odds with climate modelling. The presence of valley networks, dendritic channels and deltas on ancient terrains points towards running water

Reprints and permissions information is available at www.nature.com/reprints.

***Correspondence and requests for materials** should be addressed to J.L.B. jbishop@seti.org.

Author contributions

J.L.B. generated the idea of short-term warm and wet events, performed remote sensing of Mars using orbital visible and near-infrared spectra and wrote most of the paper.

A.G.F. contributed preliminary discussions defining the direction of the project and provided insights on the nature of the early Mars climate, thermodynamics of clay minerals and current Mars Science Laboratory rover results. J.R.M. provided analyses of Fe/Mg phyllosilicates from hydrothermal ocean environments and remote sensing results of Mars, and prepared figures. L.G.-D. conducted the clay synthesis modelling and prepared figures. L.L.B. contributed insights on basalt alteration and the formation of clays and poorly crystalline phases. M.A.V. provided insights on the weathering of Martian meteorites and basalt. C.G. prepared the HRSC and HiRISE images. E.B.R. contributed analyses of poorly crystalline phases of Mars in remote sensing thermal infrared emission orbital spectra and provided insights on current Mars Science Laboratory rover results regarding clays and poorly crystalline materials. All authors contributed to writing and commenting on drafts of the paper.

Competing interests

The authors declare no competing financial interests.

Supplementary information accompanies this paper at <https://doi.org/10.1038/s41550-017-0377-9>.

Publisher's note: Springer Nature remains neutral with regard to jurisdictional claims in published maps and institutional affiliations.

and fluvial erosion on early Mars¹, but climate modelling indicates that long-term warm conditions were not sustainable². Widespread phyllosilicates and other aqueous minerals on the Martian surface³⁻⁶ provide additional evidence that an early wet Martian climate resulted in surface weathering. Some of these phyllosilicates formed in subsurface crustal environments⁵, with no association with the Martian climate, while other phyllosilicate-rich outcrops exhibit layered morphologies and broad stratigraphies⁷ consistent with surface formation. Here, we develop a new geochemical model for early Mars to explain the formation of these clay-bearing rocks in warm and wet surface locations. We propose that sporadic, short-term warm and wet environments during a generally cold early Mars enabled phyllosilicate formation without requiring long-term warm and wet conditions. We conclude that Mg-rich clay-bearing rocks with lateral variations in mixed Fe/Mg smectite, chlorite, talc, serpentine and zeolite occurrences formed in subsurface hydrothermal environments, whereas dioctahedral (Al/Fe³⁺-rich) smectite and widespread vertical horizonation of Fe/Mg smectites, clay assemblages and sulphates formed in variable aqueous environments on the surface of Mars. Our model for aluminosilicate formation on Mars is consistent with the observed geological features, diversity of aqueous mineralogies in ancient surface rocks and state-of-the-art palaeoclimate scenarios.

The past 50 years of exploration have revealed dry river channels and related alluvial fans and deltas, all of which convincingly indicate that substantial surface water existed in the Noachian and parts of the Hesperian, over 3,500 million years ago⁸. However, increasing evidence has shown that these geomorphic features may have formed during short-lived aqueous events on what was otherwise a potentially cold, arid planet². Together with the geomorphic features, the presence of multiple types of secondary minerals (that is, phyllosilicates, sulphates, iron oxides, silica and carbonates) found throughout the ancient crust points to the interaction of liquid water with surface basalts and the ancient crust in the past³⁻⁶.

In this study, we evaluate the nature and stratigraphy of clay-bearing surface units observed on Mars, in the context of clay-forming environments on Earth, in laboratory simulations and geochemical modelling experiments, in order to provide constraints on the early Martian climate and the nature of aqueous surface environments. As different phyllosilicates form in different alteration environments⁹, we compare surface units dominated by smectite clays with those dominated by mixed-layer smectite/chlorite and other clay assemblages. Occurrences of trioctahedral (three cations per formula unit in octahedral sites; typically Mg²⁺ or Fe²⁺) and dioctahedral smectites (two cations per formula unit in octahedral sites; typically Al³⁺ or Fe³⁺) also imply different formation environments⁹.

Dioctahedral smectite occurrences are observed in layered outcrops in many Noachian and some early Hesperian terrains^{3,7} (Fig. 1a). Mg-rich trioctahedral phyllosilicate mixtures are more consistent with formation under reducing conditions in subsurface hydrothermal or metamorphic environments, or through burial diagenesis⁹. Terrestrial smectite-bearing hydrothermally altered sea-floor sediments were used to classify interstratified smectite, chlorite and talc assemblages on Mars¹⁰. Zeolite is also an indicator of deep, subsurface alteration of Columbia River basalt (CRB), where nontronite forms in all cases, but zeolite only forms at depth under elevated temperatures¹¹. Subsurface environments have been

proposed for clay formation in many locations on Mars⁵. The Northeast Syrtis region including Nili Fossae hosts several Mg-rich phyllosilicate assemblages (for example, Fe/Mg smectite, chlorite, prehnite, serpentine and talc), which occur in the basement rocks and vary across the terrain in neighbouring units^{12,13}, and this is also consistent with multiple, distinct subsurface regions controlled by different chemical environments. Some of these mixed clay assemblages may have formed in subsurface environments up to several hundred °C and are not associated with any surface environment or climate on Mars, while others are consistent with authigenic precipitation in cooler near-surface or subaerial environments⁵. Early diagenesis at relatively low temperatures in lacustrine sediments of the Yellowknife Bay formation in the Gale Crater may have also partially chloritized the pre-existing Fe saponite⁶.

In contrast, clay profiles dominated by dioctahedral smectites on Earth are typically formed in subaqueous or subaerial surface environments⁹. These temperate-to-warm climates with alternating wet ($>50 \text{ cm yr}^{-1}$) and dry seasons support soil formation with abundant smectites (up to 90% of phyllosilicates). Nontronite on Mars, occurring in wide expanses of layered material such as those observed at Mawrth Vallis (Fig. 1b), is consistent with formation in surface environments¹⁴. A common stratigraphy containing phyllosilicates, hydrated silica and sulphates is found across hundreds to thousands of km^2 in this region¹⁵. A 150–200-m-thick Fe/Mg smectite (nontronite) unit is the dominant aluminosilicate material observed here, capped by sulphates in some areas, then a 50-m-thick Al phyllosilicate or opal unit¹⁶ that is covered by poorly crystalline aluminosilicates¹⁷ (Fig. 1c). Additional outcrops containing dioctahedral smectites (Fig. 1a), Al phyllosilicates and sulphates are also present in the Northeast Syrtis region¹², on plateaus in Southeast Valles Marineris⁴ and within volcanic units at the Eridania basin in Terra Sirenum⁴, and fluviolacustrine mudstone of the 200-m-thick Murray formation at Gale Crater contains up to ~25 wt% phyllosilicate, including both dioctahedral Al-rich smectite and trioctahedral Mg-rich smectite¹⁸. We propose that dioctahedral smectite-rich outcrops and laterally extensive vertical profiles of Fe/Mg smectites, sulphates and Al-rich clay assemblages are more consistent with formation in surface environments⁹.

The common compositional stratigraphy of Al clays over Fe clays⁴ is an important constraint. During the Noachian when this alteration occurred, the Martian surface was geologically active with resurfacing by volcanism, meteor impact, and aeolian, fluvial and deltaic sedimentation. Yet, this widespread weathering profile⁴ is not disrupted in most places. While the global exposure of these sequences is surely incomplete, the general observation of a similar mineralogical stratigraphy suggests a single event or several closely spaced events of intense chemical weathering that produced surface phyllosilicates in several outcrops across Mars (Fig. 1d, model 1), rather than multiple small events spaced out over long time periods (Fig. 1d, model 2).

Amorphous and poorly crystalline materials, such as opal, nanophase aluminosilicates and ferrihydrite on the surface of Mars have been recognized recently through analysis of data from orbital¹⁹ and surface missions⁶. In the Mawrth Vallis region, this poorly crystalline material is present at 20–30 vol.% for the light-toned regions where clay minerals are detected¹⁷. An X-ray amorphous component is also present at ~20–50 wt% nearly

everywhere the Chemistry and Mineralogy (CheMin) X-ray diffractometer has analysed samples at Gale Crater⁶. These poorly crystalline or amorphous components on the Martian surface are probable markers of a relatively dry and/or cold climate, when formation of clay minerals no longer occurred. Nanophase aluminosilicates form preferentially over phyllosilicates in well-drained environments with low water-to-rock ratio systems^{20,21} and cold climates such as the Antarctic Dry Valleys²².

We show here that the types of phyllosilicate and poorly crystalline phases formed in surface environments on Mars can provide strong constraints on the climate. All else being equal, there is a tradeoff between time and temperature for the formation of clay minerals because these reactions proceed faster under warmer conditions²³. Our results offer insight into the nature of the different scenarios of cold, warm, dry, wet and icy early Mars, as follows.

First, cold scenarios have been proposed for Mars that would enable either a cold and wet^{24,25} or a cold and dry^{2,26} early Mars. Some clay minerals can form at temperatures just above freezing in an environment hosting liquid water, but the reactions would proceed extremely slowly^{23,25}. Our models of nontronite formation (Fig. 2) found almost no nontronite production near freezing, but a significant increase in the rate of reaction occurred at ~ 20 °C²⁵. Thus, for liquid water temperatures < 20 °C (or mean annual temperatures just above freezing), even sustained periods of high water-to-rock ratio were probably not sufficient to produce the observed smectite outcrops on Mars, including the ~ 200 -m-thick nontronite-rich beds at Mawrth Vallis. This scenario would require standing bodies of cold water persisting for hundreds of millions of years, which is not currently supported by climate modelling² or weathering profiles (Fig. 1d) on Mars.

Second, temperatures of 25–50 °C may have been sufficient to form the ubiquitous Fe/Mg smectite observed on Mars in geologically short periods of time. Reactions modelled at temperatures up to 40 °C here (Fig. 2) showed a continual increase in smectite crystallization, consistent with field⁹ and laboratory²⁷ observations that nontronite forms readily in the 30–75 °C range. The saponite reactions modelled here indicate that the rate of saponite formation also increases with temperature, but that crystallization may occur more rapidly for some forms of saponite compared with nontronite over the 10–30 °C range. Smectite-bearing CRB palaeosols and nontronite-rich saprolites up to several metres thick formed at mean annual temperatures of 5–11 °C on the Earth's surface in time periods of several hundred thousand years or less²⁸. Temperature also affects which types of clay minerals form. Some forms of saponite may crystallize at slightly lower temperatures than nontronite (Fig. 2), while moderately warmer conditions support the increased formation of Al phyllosilicates (Supplementary Fig. 2) and goethite⁹.

Third, indicators for environments with limited liquid water on the surface can be found in surface regions on Mars containing poorly crystalline, nanophase and amorphous materials such as allophane, imogolite, opal, ferrihydrite and schwertmannite¹⁷. The formation of allophane and imogolite from volcanic glass is favoured over smectite clay formation^{9,20,21} in either (1) a rainy, well-drained environment without standing liquid water or (2) a cold climate with temperatures near freezing that experienced standing liquid water from melting snow or ice. Thus, the presence of abundant nanophase aluminosilicates without

phyllosilicates could mark the end of the warm and wet surface conditions supporting smectite formation.

Considering analyses of these multiple lines of evidence, we propose that layered surface deposits of clay-rich materials could have formed on the surface of early Mars during geologically brief climate excursions (~1 Myr). Such short-term warm and wet deviations from a generally cold climate can aptly explain the sum of observed geological features, thick smectite beds and palaeoclimate constraints. This would entail a global mean temperature above freezing and local summer maxima of ~30–40 °C to produce abundant nontronite in surface outcrops in several locations over tens of thousands of years. Even short-lived climate excursions could have produced significant amounts of clay-rich alteration products from glass-rich volcanic or impact-generated basaltic material on Mars. Clay formation rates on Earth are commonly ~0.01 mm yr⁻¹ in many settings²⁹ and can reach as high as 0.05 mm yr⁻¹ in some regions, such as weathered tephra deposits in New Zealand²⁹. The formation of smectite beds up to 120 m thick is estimated using rates up to 0.01 mm yr⁻¹ for Mars (Fig. 3; see Methods).

Geological features marking flowing water and fluvial erosion are observed in many more locations on the surface^{1,8} than those that exhibit spectral signatures of clays and aqueous minerals³⁻⁵. For instance, alluvial fans, valley networks and dendritic channels are present in the Libya Montes region at several sites ranging in age from Noachian to Hesperian and even to Amazonian, where phyllosilicates are not observed³⁰. These features have been interpreted to be caused by periods of liquid water that did not persist long enough for clay formation³⁰. Another interpretation is that these features were shaped by cold water²⁴. This could indicate that cold and seasonally wet conditions may have been responsible for the regions bearing fluvial erosion features without the formation of phyllosilicates, while short-term warm and wet climate excursions were responsible for phyllosilicate-bearing regions.

Our analyses of the phyllosilicate record on Mars point to a scenario that accounts for substantial amounts of smectite clays in many locations, geological features resulting from liquid water across the planet and a generally cold and dry climate. We conclude that hundreds of metres of mostly dioctahedral clay-bearing materials could have formed in many places at the surface during short weathering intervals on a planet that was otherwise cold for 99% of the Noachian. The punctuated, warm environments proposed here for early Mars could have arisen from impacts³¹ or other forces.

Our resulting hypothesis for phyllosilicate formation on Mars encompasses differing geochemical conditions and clay types for subsurface and surface alteration. The occurrences of trioctahedral Mg-rich mixed clays including variations in smectite, chlorite, talc, serpentine or prehnite in nearby outcrops across the terrain probably formed in subsurface hydrothermal environments, while dioctahedral (Al/Fe³⁺-rich) smectite and widespread vertical stratigraphies of Fe/Mg smectites (nontronite and saponite), clay assemblages and sulphates formed in aqueous surface environments. Furthermore, we suggest that nanophase aluminosilicates formed from volcanic tephra in cold or low water-to-rock environments and that these materials are persistent over long periods of time in the

absence of liquid water. Clay-rich layered strata probably formed during bursts of short-lived weathering events affecting nanophase aluminosilicates and glass-rich materials.

Methods

Mars imagery.

The High Resolution Stereo Camera (HRSC) on board Mars Express is a push-broom scanning instrument using nine parallel charge-coupled device line detectors with 5,184 pixels each, mounted in the focal plane of a 175 mm Apo-Tessar lens. The unique capability of the HRSC camera is to obtain simultaneously high-resolution imagery in three-line stereo, in four colours and at five angles during a single orbit pass. The setup allows the calculation of stereoscopic digital elevation models from the imagery with a grid size of up to 50 m and the estimation of surface roughness by measuring the phase function of the surface at different angles³². Imagery with a resolution of up to 10 m and digital elevation models are later mosaiced together by bundle-block adjustment to produce quadrangle maps of Mars³³. For this investigation, only bundle-block-adjusted HRSC digital elevation models were used.

High Resolution Imaging Science Experiment (HiRISE) data were merged with HiRISE digital elevation models for Fig. 1c. Spectral data from the Compact Reconnaissance Imaging Spectrometer for Mars (CRISM) were superimposed onto HiRISE imagery to produce oblique views of mineralogy over the surface geology using the ESRI ArcGIS software package (<http://www.esri.com>).

Phyllosilicate reactions.

Kinetic calculations to determine the rate of low-temperature phyllosilicate formation were carried out using the PHREEQC 3.3.8 software from the United States Geological Survey as in previous analyses²⁵. Our model describes the precipitation of hydrated silicates in a solution resulting from the kinetic dissolution of basalt. The rock substrate is active. It continues dissolving kinetically and contributing ions to the solution throughout the process. Crystallization and dissolution are characterized by the saturation ratio of the minerals involved, which is defined for crystallization from solutions as IAP/K_s , where IAP is the ion activity product and K_s is the equilibrium constant³⁴. When an equilibrium model is used, the mass amount of a given phase that can precipitate is exclusively weighted by the supersaturation, which depends on several thermodynamic parameters such as the temperature, pressure and compositional dependence^{35,36}. For the kinetic characterization of the dissolution and precipitation of silicate minerals, the full equation used in our models includes a term for each of these three mechanisms where the calculated rate constant and the corresponding kinetic parameters are obtained using transition state theory³⁷. The reactions involving nontronite and saponite are initiated at pH 11 to simplify the reactions and mimic natural situations^{38,39}. Related reactions were performed at pH 8, which required the inclusion of carbonate in the system, and pH 6, which required a source of protons in the system, in order to test the results. Similar results were found at pH 6, 8 and 11 in terms of the effects of temperature and relative abundance of products for the phyllosilicates considered here. The reaction proceeds faster at pH 11 in our experiments, which could

indicate that somewhat longer durations of warm and wet conditions were required if the pH was lower.

Surface phyllosilicate outcrops and geological features due to water on Mars.

Fe/Mg smectite is the most common phyllosilicate observed on Mars⁴⁰ and the chemistry varies from more Fe-rich varieties, such as those observed near Mawrth Vallis, to more Mg-rich varieties, such as those observed near Nili Fossae³. The outcrop of the most abundant dioctahedral nontronite (Fe smectite) and montmorillonite (Al smectite) occurs in the Mawrth Vallis region^{7,41}. Light-toned outcrops of phyllosilicate-rich material (Supplementary Fig. 1) illustrate the widespread occurrence of aqueous alteration in this region. Example CRISM spectra from the most common phyllosilicate outcrops are presented in Supplementary Fig. 2 to demonstrate how readily these distinct units can be differentiated.

Ancient rock surfaces across Mars are marked by valley networks, dendritic channels and deltas that indicate frequent running water and fluvial erosion on early Mars⁴²⁻⁴⁴. Surface drainage features and the Mawrth Vallis channel can be observed to intersect and cut through the phyllosilicate outcrops (Supplementary Fig. 1), indicating that flowing water was present after their deposition. These later episodes of water activity may have been short-term and/or they may have been too cold to form phyllosilicates. Periodic or seasonal melting of snow to produce icy conditions where liquid water could carve out the observed Martian surface features has been proposed^{2,26,45,46}; however, these short-term icy conditions would be insufficient for formation of the observed phyllosilicates²⁵. These intriguing drainage and erosional features at Mawrth Vallis (Supplementary Fig. 1), coupled with multiple formation environments for the phyllosilicates and sulphates observed here¹⁴, underlie the reasoning for selecting this region as a candidate landing site for ExoMars⁴⁷.

Characterization of amorphous and poorly crystalline materials on Mars.

Amorphous and poorly crystalline aluminosilicates have been identified from orbit at Mars^{17,19,48} using the CRISM⁴⁹ and Thermal Emission Spectrometer⁵⁰ instruments. These studies found allophane and related poorly crystalline materials in several locations across the surface of Mars through modelling of Thermal Emission Spectrometer data¹⁹, Fe-rich allophane in isolated occurrences in Coprates Chasma⁴⁸ and poorly crystalline aluminosilicates in the topmost stratigraphical unit of the phyllosilicate-bearing outcrops at Mawrth Vallis¹⁷. The phyllosilicate stratigraphy at Mawrth Vallis contains several different units vertically through the profile^{14,17} and is consistent with deposition, leaching or pedogenesis on the surface^{7,51}.

The CheMin instrument on the Mars Science Laboratory rover employs X-ray diffraction for characterization of minerals at Gale Crater⁵². A broad X-ray diffraction hump in these data is used to quantify the amorphous and poorly crystalline phases⁵². FULLPAT analyses of the CheMin data have determined that ~20–50 wt% of the materials studied are amorphous or poorly crystalline^{6,53}. Coordinating these CheMin results with the volatile components identified by the Sample Analysis at Mars instrument and the bulk geochemistry measured

by the Alpha Particle X-ray Spectrometer indicates that the X-ray amorphous material at Gale Crater is likely a mixture of aluminosilicates, sulphates and iron oxides⁵⁴.

Environmental constraints on phyllosilicate and poorly crystalline aluminosilicate formation.

Allophane and related aluminosilicates transform preferentially to clays through the alteration of volcanic ash in low-temperature environments or regions with high drainage²⁰. Allophane and imogolite have been well-characterized in rainy low water-to-rock ratio systems in Japan^{55,56}, New Zealand⁵⁷, Ecuador⁵⁸ and the Hawaiian islands^{59,60}. Laboratory syntheses of these nanophase aluminosilicates are typically performed at a pH of ~4–5 and 20–100 °C for a few days (see, for example, refs ⁶¹⁻⁶⁴). These mildly acidic conditions favour dissolution of the glass or silicates and, as the nanophase aluminosilicates are formed, the pH typically becomes neutral to slightly alkaline. Nanophase aluminosilicates are also observed as alteration products in several cold environments, such as glacial deposits in Oregon⁶⁵, in cold streams in Iceland⁶⁶, at high elevation in the Cascade mountain range in California²¹ and in sediments in the Antarctic Dry Valleys²². Alteration of volcanic glass in cold environments results in nanophase aluminosilicates and poorly crystalline phyllosilicates. This is also observed in phyllosilicate synthesis, where the reactions proceed extremely slowly at low temperature and the products remain poorly crystalline or impure^{23,25,67,68}. Laboratory experiments also showed that nanophase Fe³⁺/Si oxides remain as short-range ordered materials and do not crystallize to clay minerals⁶⁸. Short-range ordered aluminosilicates and iron oxides and hydroxides have been observed in Martian meteorites as well^{69,70}, and continued investigation of these materials may also provide insights into the poorly crystalline materials on the surface of Mars.

Aqueous alteration of olivine in Martian meteorites proceeds exceedingly slowly upon exposure to thin films of brine under cold, dry Antarctic conditions; however, olivine alteration and clay formation may occur over durations as brief as centuries or even decades of episodic wetting exposure under more moderate temperatures and under acidic pH conditions^{71,72}. For some basaltic materials, alteration to form poorly crystalline aluminosilicates and Fe³⁺ species can proceed over a period of months⁷³.

Some constraints exist on the formation time and conditions of secondary mineral assemblages found in Martian meteorites and considered to be of Martian origin⁷⁴. The lack of O isotopic equilibrium suggests temperatures <150 °C. It has been suggested that the presence of metastable carbonate phases indicates rapid precipitation of the secondary phases, probably under conditions of transient wetting on a timescale of perhaps days. However, these assemblages constitute 1 vol.% or less of the host rock and may not be indicative of rates for more extensively altered material.

Estimating phyllosilicate formation rates on Mars.

Factors such as temperature, water-to-rock ratio and silica activity affect phyllosilicate formation (see, for example, refs ^{9,23,67}). Smectite formation experiments in the laboratory have shown that low-temperature reactions proceed very slowly and the products are impure or poorly crystalline minerals^{23,67,68}. More recent nontronite synthesis experiments showed

that samples prepared hydrothermally from a gel in air at 75–150 °C were similar to each other in purity and form, regardless of the synthesis temperature²⁷. Thus, temperatures over 75 °C were probably not necessary for abundant nontronite formation on Mars, and modelling suggests that temperatures in the range 20–40 °C (Fig. 2) should have been sufficient over geological timescales to form the observed nontronite occurrences on Mars in locations such as Mawrth Vallis where nontronite units are 150–200 m thick¹⁶. Nontronite has also precipitated in warm (56 °C) waters of the Red Sea to form a nontronite-rich bed several metres thick and tens of kilometres across⁷⁵. These local maximum temperatures may correspond to mean annual temperatures in the range 5–20 °C.

Nontronite is the first alteration product of CRB and is stable under ambient conditions in the basalt-hosted aquifer¹¹. Nontronite also fills cracks and void spaces in surface basalt flows⁷⁶. Experimentally measured crystallization rates suggest that these clays may form slowly, over timescales of up to millions of years⁷⁷. Stacked CRB flows of the Grande Ronde and Wanapum basalts (14.5–16 million years ago) contain palaeosols composed of kaolinite or montmorillonite soils overlying nontronite-bearing basalt saprolites^{28,78–80}. These soils formed by weathering under the relatively warm and wet conditions of the mid-Miocene climatic optimum, with annual precipitation of 230–1,200 mm, mean annual temperatures of 7–16 °C and wet summer conditions^{79,81}. The degree of weathering and soil development varied with climatic conditions, which in turn varied with both time²⁸ and location/elevation⁸¹. Palaeosols weathered under warmer conditions contain kaolinite, whereas those weathered under cooler conditions are dominated by montmorillonite²⁸. Palaeoprecipitation amounts were a major factor in controlling the extent of weathering and soil development, whereas the duration of weathering was not⁷⁷. In western Oregon, wetter conditions led to more intensive weathering and the formation of thick bauxite deposits^{82,83}.

The absence of palaeosols on the uppermost capping CRB flows in most locations suggests that intensive weathering may have ended with the end of the mid-Miocene climatic optimum. However, another study showed that secondary minerals equilibrated after the basalts cooled and that nontronite formation ought to be ongoing, if slow, in the aquifer⁸⁴. The dependence of weathering intensity on temperature as well as precipitation suggests that the end of wet summer conditions in the region may have been a primary factor affecting basalt weathering, but this hypothesis has not yet been tested.

Models of nontronite formation found almost no nontronite production near freezing, with an increase in the rate of the reaction near ~20 °C²⁵. Reactions modelled here at temperatures up to 40 °C (Fig. 2) showed a continual increase in nontronite crystallization (Fig. 2), consistent with field and laboratory observations that nontronite forms readily in the 30–75 °C range. The saponite reactions modelled here indicate that the rate of saponite formation also increases with temperature, but that crystallization may occur more rapidly for some forms of saponite compared with nontronite over the 10–30 °C range (Fig. 2). Mixed Fe/Mg phyllosilicates containing smectite and chlorite or smectite, serpentine, talc and prehnite assemblages are formed at elevated temperatures (>120°C) via hydrothermal alteration or burial diagenesis^{9,85}, which supports subsurface formation of these mixed clay assemblages on Mars. Regions of carbonate and smectite⁸⁶, saponite and chlorite¹², saponite and serpentine⁸⁷ or talc and saponite^{13,88} in the Northeast Syrtis region of Mars are

examples of these subsurface crustal clays. Subsequent surface alteration in this area at the Nochian–Hesperian boundary produced a variety of phyllosilicates and sulphates⁸⁹.

Near-surface burial diagenesis has also probably occurred on sedimentary smectites at many locations on Mars. For example, beidellite has been observed instead of montmorillonite in clay outcrops around Isidis Basin^{30,90} and illite and chlorite have been observed in the Nili Fossae region⁵. These clay minerals could be formed through burial diagenesis in the transition from montmorillonite to beidellite that occurs during the initial phase of illitization. Continued diagenesis can form chlorite⁹¹ or muscovite⁹². This clay transformation is supported by laboratory experiments where montmorillonite was converted to beidellite and illite over the temperature range 100–200°C⁹³.

Characterization of the phyllosilicates at Gale Crater indicate that low-temperature diagenesis occurred with temperatures below ~75 °C^{53,94}. These studies are consistent with the formation of clay minerals after deposition but before lithification (that is, in early diagenetic environments). Diagenesis of sediments at Gale Crater could have been supported by post-impact heat from the impact^{95,96}. Fluid modelling of Gale Crater mudstones in these studies resulted in Mg nontronite, chlorite and serpentine chemistries similar to those observed at Yellowknife Bay.

Low-temperature smectite synthesis experiments indicate that montmorillonite formation is significantly slower than nontronite formation⁶⁸. This could explain why Fe/Mg smectite outcrops are more common and typically thicker on Mars than Al smectite occurrences⁴. Crystallization experiments were performed for Al phyllosilicates (Supplementary Fig. 3) similarly to those of Fe/Mg smectites (Fig. 2). The rate expressions were based on the results of previous studies^{38,39} and take into account the effect of Al³⁺ speciation on the precipitation rate.

Other factors strongly affecting phyllosilicate formation rates are the composition and physical form of the protolith (see, for example, refs ^{9,97}). Clay formation rates of ~0.001–0.1 g kg⁻¹ yr⁻¹ were observed from New Zealand tephras, where the rock type, pH and drainage were important factors⁹⁷. Phyllosilicate formation rates depend on how fast the rock weathers, making the cations and anions available for clay formation. Weathering rates are generally higher in more fragmented materials and for more mafic rocks. Given that mafic and ultramafic volcanoes would be more explosive on Mars than Earth⁹⁸, the Martian surface would have contained large amounts of highly reactive, draping deposits of volcanic and impact-generated glassy materials. Such hyaloclastites react more quickly to form phyllosilicates or nanophase aluminosilicates, depending on the aqueous environment and temperature (see, for example, ref. ⁹).

Even short-lived warm and wet climate excursions could have produced significant amounts of clay-rich alteration products from a hyaloclastite protolith. Smectite occurs in the greatest abundance on Earth in arid, tropical regions where it rains during the warm season. If mechanisms can be found to explain sufficiently warm and wet environments (locally 40–50 °C with 100 cm yr⁻¹ rain or perhaps mean annual temperatures of 10–15 °C), Mars need

not have been warm and wet for long periods of time in order to have formed the observed mineralogy.

Changes in obliquity⁹⁹ have been suggested as a way to warm Mars sufficiently to melt the ice and produce liquid water that could cause the water-driven features observed on the surface. Obliquity studies have typically only discussed the need for liquid water. Perhaps future studies can find mechanisms for heating the planet further to 10–15 °C mean annual temperatures or locally during summer to 40–50 °C. Other possible events to produce short-term warming of the planet to these temperatures could include geothermal activity¹⁰⁰, large impacts³¹ or methane bursts¹⁰¹.

Data availability.

The data that support the findings of this study are available from the corresponding author upon reasonable request.

Supplementary Material

Refer to Web version on PubMed Central for supplementary material.

Acknowledgements

The authors are grateful for support from the National Aeronautics and Space Administration Astrobiology Institute (grant NNX15BB01 to J.L.B.) and Mars Data Analysis Program (grant NNX12AJ33G to J.L.B.), as well as the project 'icyMARS', European Research Council Starting Grant 307496 (to A.G.F.), a Smithsonian Senior Fellowship (to M.A.V.) and Deutsches Zentrum für Luft- und Raumfahrt grant 50QM1702 'HRSC on Mars Express' on behalf of the German Federal Ministry for Economic Affairs and Energy (to C.G.). The authors also thank L. Maltagliati, J. W. Head, J. F. Mustard and S. Clifford for helpful comments that improved the manuscript.

References

1. Hynek BM, Beach M & Hoke MRT Updated global map of Martian valley networks and implications for climate and hydrologic processes. *J. Geophys. Res.* 115, E09008 (2010).
2. Wordsworth R et al. Transient reducing greenhouse warming on early Mars. *Geophys. Res. Lett.* 44, 665–671 (2017).
3. Murchie SL et al. A synthesis of Martian aqueous mineralogy after 1 Mars year of observations from the Mars Reconnaissance Orbiter. *J. Geophys. Res.* 114, E00D06 (2009).
4. Carter J, Loizeau D, Mangold N, Poulet F & Bibring J-P Widespread surface weathering on early Mars: a case for a warmer and wetter climate. *Icarus* 248, 373–382 (2015).
5. Ehlmann BL et al. Subsurface water and clay mineral formation during the early history of Mars. *Nature* 479, 53–60 (2011). [PubMed: 22051674]
6. Vaniman DT et al. Mineralogy of a mudstone at Yellowknife Bay, Gale Crater, Mars. *Science* 343, 1243480 (2014). [PubMed: 24324271]
7. Bishop JL et al. Phyllosilicate diversity and past aqueous activity revealed at Mawrth Vallis, Mars. *Science* 321, 1159830–1159833 (2008).
8. Fassett CI & Head JW Valley network-fed, open-basin lakes on Mars: distribution and implications for Noachian surface and subsurface hydrology. *Icarus* 198, 37–56 (2008).
9. Chamley H *Clay Sedimentology* (Springer, Berlin, Germany, 1989).
10. Michalski JR et al. Constraints on the crystal-chemistry of Fe/Mg-rich smectitic clays on Mars and links to global alteration trends. *Earth Planet. Sci. Lett.* 427, 215–225 (2015).
11. Benson LV & Teague LS Diagenesis of basalts from the Pasco Basin, Washington—I. Distribution and composition of secondary mineral phases. *J. Sediment. Res.* 52, 595–613 (1982).

12. Ehlmann BL et al. Identification of hydrated silicate minerals on Mars using MRO-CRISM: geologic context near Nili Fossae and implications for aqueous alteration. *J. Geophys. Res.* 114, E00D08 (2009).
13. Viviano CE, Moersch JE & McSween HY Implications for early hydrothermal environments on Mars through the spectral evidence for carbonation and chloritization reactions in the Nili Fossae region. *J. Geophys. Res.* 118, 1858–1872 (3013).
14. Bishop JL et al. What the ancient phyllosilicates at Mawrth Vallis can tell us about possible habitability on early Mars. *Planet. Space Sci.* 86, 130–149 (2013).
15. Noe Dobrea EZ et al. Mineralogy and stratigraphy of phyllosilicate-bearing and dark mantling units in the greater Mawrth Vallis/west Arabia Terra area: constraints on geological origin. *J. Geophys. Res.* 115, E00D19 (2010).
16. Loizeau D et al. Stratigraphy in the Mawrth Vallis region through OMEGA, HRSC color imagery and DTM. *Icarus* 205, 396–418 (2010).
17. Bishop JL & Rampe EB Evidence for a changing Martian climate from the mineralogy at Mawrth Vallis. *Earth Planet. Sci. Lett.* 448, 42–48 (2016).
18. Bristow TF. Surveying clay mineral diversity in the Murray formation, Gale Crater, Mars; *Proc. 48th Lunar Planet. Sci. Conf*; 2017.
19. Rampe EB et al. Allophane detection on Mars with Thermal Emission Spectrometer data and implications for regional-scale chemical weathering processes. *Geology* 40, 995–998 (2012).
20. Parfitt RL Allophane and imogolite: role in soil biogeochemical processes. *Clay Miner.* 44, 135–155 (2009).
21. Rasmussen C, Dahlgren RA & Southard RJ Basalt weathering and pedogenesis across an environmental gradient in the southern Cascade Range, California, USA. *Geoderma* 154, 473–485 (2010).
22. Bishop JL et al. Mineralogical analyses of surface sediments in the Antarctic Dry Valleys: coordinated analyses of Raman spectra, reflectance spectra and elemental abundances. *Phil. Trans. R. Soc. A* 372, 20140198 (2014). [PubMed: 25368345]
23. Klopogge JT, Komarneni S & Amonette J Synthesis of smectite clay minerals: a critical review. *Clays Clay Miner.* 47, 529–554 (1999).
24. Fairén AG A cold and wet Mars. *Icarus* 208, 165–175 (2010).
25. Fairén AG et al. Cold glacial oceans would have inhibited phyllosilicate sedimentation on early Mars. *Nat. Geosci.* 4, 667–670 (2011).
26. Head JW & Marchant DR The climate history of early Mars: insights from the Antarctic McMurdo Dry Valleys hydrologic system. *Antarct. Sci.* 26, 774–800 (2014).
27. Decarreau A, Petit S, Martin F, Vieillard P & Joussein E Hydrothermal synthesis, between 75 and 150°C, of high-charge ferric nontronites. *Clays Clay Miner.* 56, 322–337 (2008).
28. Hobbs KM & Parrish JT Miocene global change recorded in Columbia River basalt-hosted paleosols. *Geol. Soc. Am. Bull.* 128, 1543–1554 (2016).
29. Price JR, Velbel MA & Patino LC Rates and time scales of clay-mineral formation by weathering in saprolitic regoliths of the southern Appalachians from geochemical mass balance. *Geol. Soc. Am. Bull.* 117, 783–794 (2005).
30. Bishop JL et al. Mineralogy and morphology of geologic units at Libya Montes, Mars: ancient aqueous outcrops, mafic flows, fluvial features and impacts. *J. Geophys. Res.* 118, 487–513 (2013).
31. Segura TL, Toon OB, Colaprete A & Zahnle K Environmental effects of large impacts on Mars. *Science* 298, 1977–1980 (2002). [PubMed: 12471254]
32. Gwinner K et al. The High Resolution Stereo Camera (HRSC) of Mars Express and its approach to science analysis and mapping for Mars and its satellites. *Planet. Space Sci.* 126, 93–138 (2016).
33. Michael GG et al. Systematic processing of Mars Express HRSC panchromatic and colour image mosaics: image equalisation using an external brightness reference. *Planet. Space Sci.* 121, 18–26 (2016).
34. Blum AE & Stillings LL in *Chemical Weathering Rates of Silicate Minerals* Vol. 31 (eds White AF & Brantley SL) 291–352 (Mineralogical Society of America, Washington DC, USA, 1995).

35. Dove PM in *Chemical Weathering Rates of Silicate Minerals Vol. 31* (eds White AF & Brantley SL) 235–290 (Mineralogical Society of America, Washington DC, USA, 1995).
36. Köhler SJ, Bosbach D & Oelkers EH Do clay mineral dissolution rates reach steady state? *Geochim. Cosmochim. Acta* 69, 1997–2006 (2005).
37. Aagaard P & Helgeson HC Thermodynamic and kinetic constraints on reaction rates among minerals and aqueous solutions. I. Theoretical considerations. *Am. J. Sci.* 282, 237–285 (1982).
38. Sverdrup H & Warfvinge P in *Chemical Weathering Rates of Silicate Minerals Vol. 31* (eds White AF & Brantley SL) 485–542 (Mineralogical Society of America, Washington DC, USA, 1995).
39. Palandri JL & Kharaka YK *A Compilation of Rate Parameters of Water-Mineral Interaction Kinetics for Application to Geochemical Modeling* (US Department of the Interior & US Geological Survey, Menlo Park, CA, 2004).
40. Mustard JF et al. Hydrated silicate minerals on Mars observed by the Mars Reconnaissance Orbiter CRISM instrument. *Nature* 454, 305–309 (2008). [PubMed: 18633411]
41. Poulet F et al. Phyllosilicates on Mars and implications for early Martian climate. *Nature* 438, 623–627 (2005). [PubMed: 16319882]
42. Ansan V, Mangold N, Masson P, Gailhardis E & Neukum G Topography of valley networks on Mars from Mars Express High Resolution Stereo Camera digital elevation models. *J. Geophys. Res.* 113, E07006 (2008).
43. Fassett CI & Head JW Sequence and timing of conditions on early Mars. *Icarus* 211, 1204–1214 (2011).
44. Craddock RA & Howard AD The case for rainfall on a warm, wet early Mars. *J. Geophys. Res.* 107, 21-1–21-36 (2002).
45. Squyres SW & Kasting JF Early Mars: how warm and how wet? *Science* 265, 744–749 (1994). [PubMed: 11539185]
46. Head JW. Late Noachian climate of Mars: Constraints from valley network system formation times and the intermittencies (episodic/periodic and punctuated); *Proc. 48th Lunar Planet. Sci. Conf.*; 2017.
47. Gross C. Mawrth Vallis—an auspicious destination for the ESA and NASA 2020 landers; *Proc. 48th Lunar Planet. Sci. Conf.*; 2017.
48. Weitz CM, Bishop JL, Baker LL & Berman DC Fresh exposures of hydrous Fe-bearing amorphous silicates on Mars. *Geophys. Res. Lett.* 41, 8744–8751 (2014).
49. Murchie SL et al. The Compact Reconnaissance Imaging Spectrometer for Mars investigation and data set from the Mars Reconnaissance Orbiter’s primary science phase. *J. Geophys. Res.* 114, E00D07 (2009).
50. Christensen PR et al. Mars Global Surveyor Thermal Emission Spectrometer experiment: investigation description and surface science results. *J. Geophys. Res.* 106, 23823–23871 (2001).
51. McKeown NK et al. Characterization of phyllosilicates observed in the central Mawrth Vallis region, Mars, their potential formational processes, and implications for past climate. *J. Geophys. Res.* 114, E00D10 (2009).
52. Blake DF et al. Curiosity at Gale Crater, Mars: characterization and analysis of the Rocknest sand shadow. *Science* 341, 1239505 (2013). [PubMed: 24072928]
53. Bristow TF et al. The origin and implications of clay minerals from Yellowknife Bay, Gale Crater, Mars. *Am. Mineral.* 100, 824–836 (2015). [PubMed: 28798492]
54. Ming DW et al. Volatile and organic compositions of sedimentary rocks in Yellowknife Bay, Gale Crater, Mars. *Science* 343, 1245267 (2014). [PubMed: 24324276]
55. Henmi T & Wada K Morphology and composition of allophane. *Am. Mineral.* 61, 379–390 (1976).
56. Bishop JL et al. Spectral and hydration properties of allophane and imogolite. *Clays Clay Miner.* 61, 57–74 (2013).
57. Parfitt RL & Henmi T Structure of some allophanes from New Zealand. *Clays Clay Miner.* 28, 285–294 (1980).
58. Kaufhold S et al. A new massive deposit of allophane raw material in Ecuador. *Clays Clay Miner.* 57, 72–81 (2009).

59. Wada K, Henmi T, Yoshinaga N & Patterson SH Imogolite and allophane formed in saprolite of basalt on Maui, Hawaii. *Clays Clay Miner.* 20, 375–380 (1972).
60. Parfitt RL, Childs CW & Eden DN Ferrihydrite and allophane in four andepts from Hawaii and implications for their classification. *Geoderma* 41, 223–241 (1988).
61. Farmer VC, Adams MJ, Fraser AR & Palmieri F Synthetic imogolite: properties, synthesis, and possible applications. *Clay Miner.* 18, 459–472 (1983).
62. Wada SI, Eto A & Wada K Synthetic allophane and imogolite. *J. Soil. Sci.* 30, 347–355 (1979).
63. Abidin Z, Matsue N & Henmi T Differential formation of allophane and imogolite: experimental and molecular orbital study. *J. Comput. Aided Mater. Des.* 14, 5–18 (2007).
64. Baker LL, Nickerson RD & Strawn DG XAFS study of Fe-substituted allophane and imogolite. *Clays Clay Miner.* 62, 20–34 (2014).
65. Scudder NA, Horgan B, Rutledge AM & Rampe EB Using composition to trace glacial, fluvial, and aeolian sediment transport in a Mars-analog glaciated volcanic system. In *Proc. 48th Lunar Planet. Sci. Conf.* 2625 (2017).
66. Thorpe MT, Hurowitz JA & Dehouck E A frigid terrestrial analog for the paleoclimate of Mars. In *Proc. 48th Lunar Planet. Sci. Conf.* 2599 (2017).
67. Eberl DD, Farmer VC & Barrer RM Clay mineral formation and transformation in rocks and soils [and discussion]. *Philos. Trans. R. Soc. Lond. A* 311, 241–257 (1984).
68. Harder H Synthesis of iron layer silicate minerals under natural conditions. *Clays Clay Miner.* 26, 65–72 (1978).
69. McKay DS et al. Search for past life on Mars: possible relic biogenic activity in Martian meteorite ALH 84001. *Science* 273, 924–930 (1996). [PubMed: 8688069]
70. Hicks LJ, Bridges JC & Gurman SJ Ferric saponite and serpentine in the nakhlite Martian meteorites. *Geochim. Cosmochim. Acta* 136, 194–210 (2014).
71. Velbel MA Aqueous corrosion of olivine in the Mars meteorite Miller Range (MIL) 03346 during Antarctic weathering: implications for water on Mars. *Geochim. Cosmochim. Acta* 180, 126–145 (2016).
72. Hallis LJ, Ishii HA, Bradley JP & Taylor GJ Transmission electron microscope analyses of alteration phases in Martian meteorite MIL 090032. *Geochim. Cosmochim. Acta* 134, 275–288 (2014).
73. Schwenzer SP. Diagenesis on Mars: Insights into noble gas pathways and newly formed mineral assemblages from long term experiments; *Proc. 48th Lunar Planet. Sci. Conf.*; 2017.
74. Bridges JC et al. Alteration assemblages in Martian meteorites: implications for near-surface processes. *Space Sci. Rev.* 96, 365–392 (2001).
75. Bischoff JL A ferroan nontronite from the Red Sea geothermal system. *Clays Clay Miner.* 20, 217–223 (1972).
76. Allen VT & Scheid VE Nontronite in the Columbia River region. *Am. Mineral.* 31, 294–312 (1946).
77. Baker LL & Strawn DG Temperature effects on the crystallinity of synthetic nontronite and implications for nontronite formation in Columbia River basalts. *Clays Clay Miner.* 62, 89–101 (2014).
78. Thomson BJ et al. The effects of weathering on the strength and chemistry of Columbia River basalts and their implications for Mars Exploration Rover Rock Abrasion Tool (RAT) results. *Earth Planet. Sci. Lett.* 400, 130–144 (2014).
79. Sheldon ND Using paleosols of the Picture Gorge basalt to reconstruct the middle Miocene climatic optimum. *PaleoBios* 26, 27–36 (2006).
80. Baker LL Formation of the ferruginous smectite Swa-1 by alteration of soil clays. *Am. Mineral.* 102, 33–41 (2017).
81. Takeuchi A, Larson PB & Suzuki K Influence of paleorelief on the mid-Miocene climate variation in southeastern Washington, northeastern Oregon, and western Idaho, USA. *Palaeogeogr. Palaeoclimatol. Palaeoecol.* 254, 462–476 (2007).
82. Allen VT Formation of bauxite from basaltic rocks of Oregon. *Econ. Geol.* 43, 619–626 (1948).

83. Liu X-M, Rudnick RL, McDonough WF & Cummings ML Influence of chemical weathering on the composition of the continental crust: insights from Li and Nd isotopes in bauxite profiles developed on Columbia River basalts. *Geochim. Cosmochim. Acta* 115, 73–91 (2013).
84. Hearn PP Jr, Steinkampf WC, White LD & Evans JR in *Safe Disposal of Radionuclides in Low-Level Radioactive Waste Repository Sites: Low-Level Radioactive Waste Disposal Workshop* (eds Bedinger MS & Stevens PR) 63–68 (US Geological Survey, Washington DC, USA, 1988).
85. Ryan PC & Hillier S Berthierine/chamosite, corrensite, and discrete chlorite from evolved verdine and evaporite-associated facies in the Jurassic Sundance Formation, Wyoming. *Am. Mineral.* 87, 1607–1615 (2002).
86. Ehlmann BL et al. Orbital identification of carbonate-bearing rocks on Mars. *Science* 322, 1828–1832 (2008). [PubMed: 19095939]
87. Ehlmann BL, Mustard JF & Murchie SL Geologic setting of serpentine deposits on Mars. *Geophys. Res. Lett.* 37, L06201 (2010).
88. Brown AJ et al. Hydrothermal formation of clay-carbonate alteration assemblages in the Nili Fossae region of Mars. *Earth Planet. Sci. Lett.* 297, 174–182 (2010).
89. Ehlmann BL & Mustard JF An in-situ record of major environmental transitions on early Mars at Northeast Syrtis Major. *Geophys. Res. Lett.* 39, L11202 (2012).
90. Bishop JL, Gates WP, Makarewicz HD, McKeown NK & Hiroi T Reflectance spectroscopy of beidellites and their importance for Mars. *Clays Clay Miner.* 59, 376–397 (2011).
91. Guisseau D et al. Significance of the depth-related transition montmorillonite-beidellite in the Bouillante geothermal field (Guadeloupe, Lesser Antilles). *Am. Mineral.* 92, 1800–1813 (2007).
92. Meunier A & Velde B *Illite: Origins, Evolution and Metamorphism* (Springer, Berlin, Germany, 2004).
93. Beaufort D, Berger G, Lachapagne JC & Meunier A An experimental alteration of montmorillonite to a di + trioctahedral smectite assemblage at 100 and 200°C. *Clay Miner.* 36, 211–225 (2001).
94. Hurowitz JA et al. Redox stratification of an ancient lake in Gale Crater, Mars. *Science* 356, eaah6849 (2017). [PubMed: 28572336]
95. Bridges JC et al. Diagenesis and clay mineral formation at Gale Crater, Mars. *J. Geophys. Res. Planets* 120, 1–19 (2015). [PubMed: 26213668]
96. Schwenzer SP et al. Fluids during diagenesis and sulfate vein formation in sediments at Gale Crater, Mars. *Meteorit. Planet. Sci.* 51, 2175–2202 (2016).
97. Lowe DJ in *Rates of Chemical Weathering of Rocks and Minerals* (eds Colman SM & Dethier DP) 265–329 (Academic Press, New York, USA, 1986).
98. Wilson L & Head JW Explosive volcanic eruptions on Mars: tephra and accretionary lapilli formation, dispersal and recognition in the geologic record. *J. Volcanol. Geotherm. Res.* 163, 83–97 (2007).
99. Laskar J et al. Long term evolution and chaotic diffusion of the insolation quantities of Mars. *Icarus* 170, 343–364 (2004).
100. Jakosky BM & Phillips RJ Mars' volatile and climate history. *Nature* 412, 237–244 (2001). [PubMed: 11449285]
101. Kite ES et al. Methane bursts as a trigger for intermittent lake-forming climates on post-Noachian Mars. *Nat. Geosci.* 10, 737–740 (2017).
102. Tanaka KL, Robbins SJ, Fortezzo CM, Skinner JA & Hare TM The digital global geologic map of Mars: chronostratigraphic ages, topographic and crater morphologic characteristics, and updated resurfacing history. *Planet. Space Sci.* 95, 11–24 (2014).

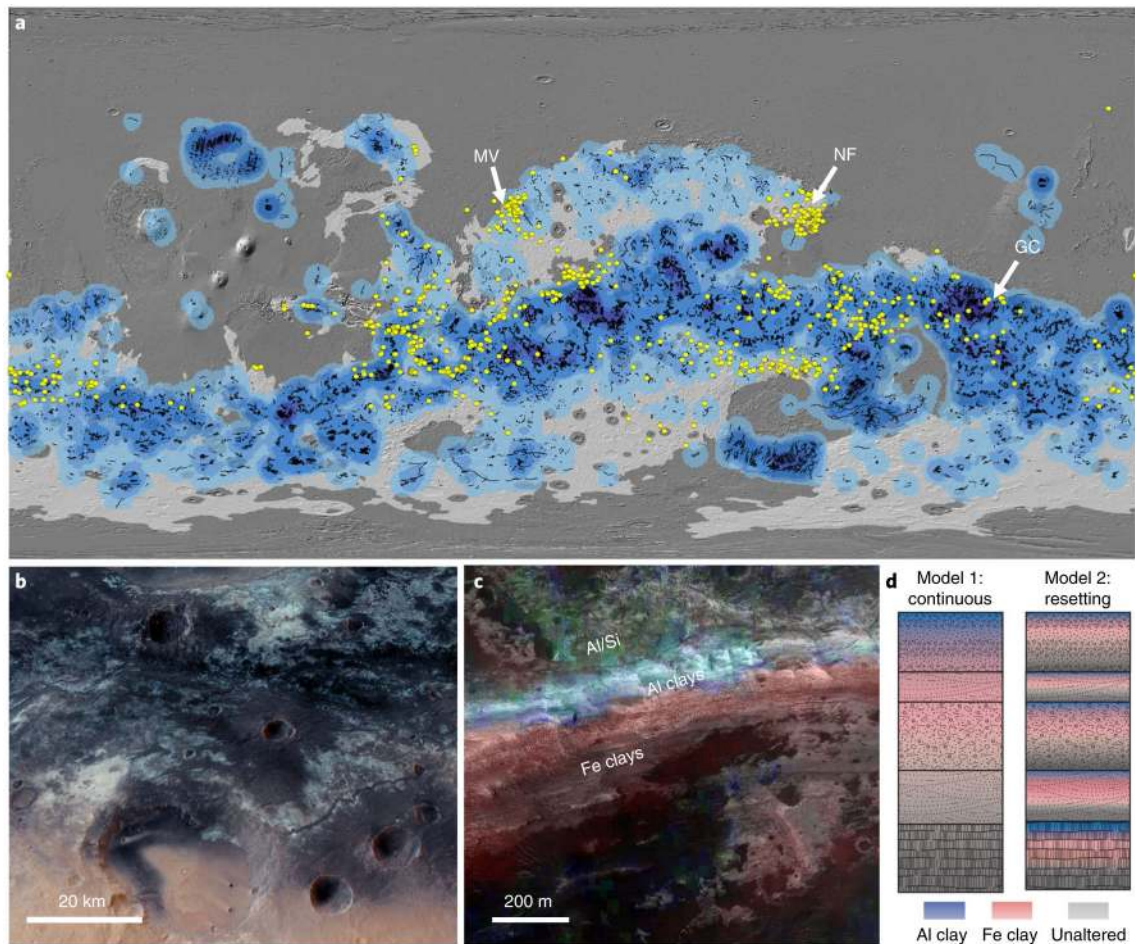


Fig. 1 |. Phyllosilicate-rich terrains on Mars.

a, Noachian terrains (white)¹⁰² contain most occurrences of valley networks (blue tones)¹ viewed over Mars Orbiter Laser Altimeter hillshade (grey). Dioctahedral smectite clays detected from orbit (yellow)¹⁰ and the locations of Mawrth Vallis (MV), Nili Fossae (NF) and Gale Crater (GC) are indicated on the map. **b**, HRSC oblique colour view demonstrating the breadth of light-toned phyllosilicate-rich material and fluvial surface features at Mawrth Vallis (5 × vertical). **c**, View of a Crater wall at Mawrth Vallis from HiRISE image PSP_004052_2045 over an HRSC digital terrain model with mineralogy from CRISM image FRT000094F6 (Fe-rich smectite, red; Al phyllosilicates, blue; allophane, green) illustrating the presence of Al clays over Fe-rich smectites. **d**, Schematic models of weathering and clay formation in surface outcrops both for the case of somewhat continuous alteration (model 1) and for alteration occurring over long time periods in a dynamic environment where the clay mineralogy is frequently reset to form alternating horizons (model 2).

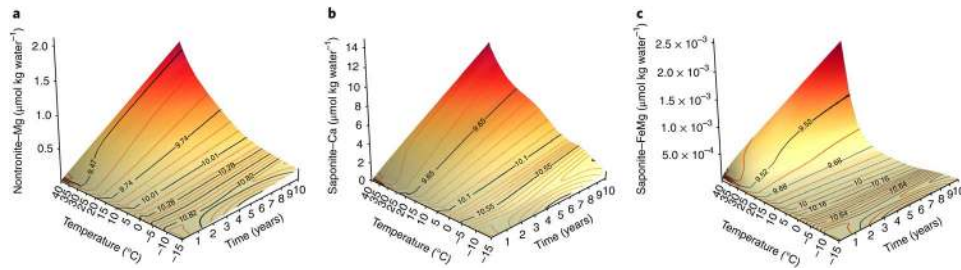


Fig. 2 |. Formation rates of smectites on Mars.

The crystallization kinetics of smectites induced by the dissolution of basalt vary greatly from temperatures near freezing to temperatures elevated to only 20–40 °C. Nontronite and saponite formation proceed increasingly rapidly for temperatures near 30–40 °C. The quantity of these smectites produced at low temperatures depends on model parameters and the type of interlayer cation. **a**, Nontronite with interlayer Mg forms at similar rates to other forms of nontronite. **b,c**, Saponite with interlayer Ca (**b**) forms much faster than saponite with interlayer Fe/Mg (**c**). The reactions are initiated at pH 11 and the evolution of pH is shown by black curves as it decreases with smectite formation (in $\mu\text{mol kg water}^{-1}$). An Fe/Mg smectite intermediate between nontronite and saponite is most common on Mars and would have progressed via similar reactions; that is, much faster for temperatures in the 30–40 °C range than near freezing. Pure smectites in both the trioctahedral saponite and dioctahedral nontronite forms would be consistent with our surface formation model; however, saponite intermixed with other trioctahedral Fe/Mg clays probably formed on Mars in much warmer subsurface environments.

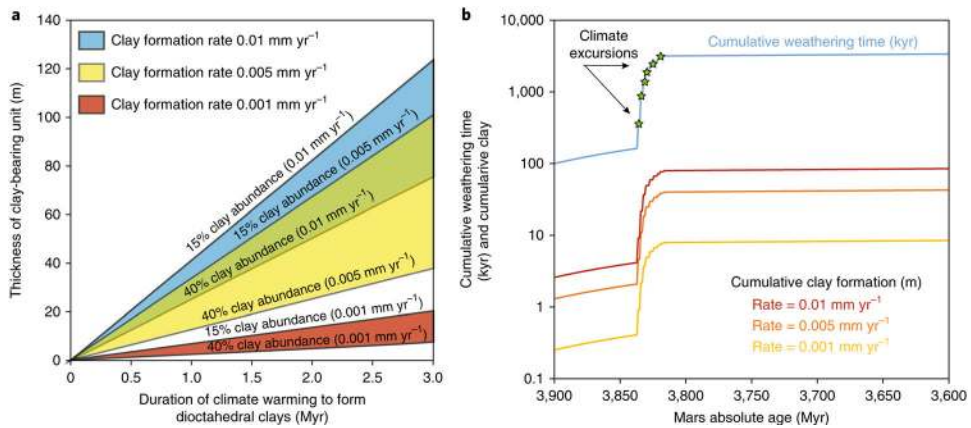


Fig. 3 | Climate excursions and surface weathering on Mars.

a, Tens to hundreds of metres of clay-rich material could have formed at the surface of Mars during short-lived climate excursions (each tens of thousands of years) spread over hundreds of millions of years. Three clay formation rates are considered from 0.001–0.01 mm yr⁻¹, which are reasonable for ultramafic, glass-bearing materials²⁹. Under the scenario shown, the total ‘chemical weathering’ time would only amount to a small fraction (<0.2%) of the Noachian period on Mars. The weathering rates used here are derived from absolute mass estimates of clay formation (g kg⁻¹) in tephra and therefore, considering that the ‘clay-rich’ deposits on Mars are likely to contain at most 50% phyllosilicates, the required durations are cut by at least half, making the already plausible scenario even easier to accomplish. **b**, Illustration of weathering progress including three million years of closely spaced climate spikes within the timeframe of 3.80–3.85 billion years ago.